Biochemical and Biophysical Research Communications 451 (2014) 246–251

Contents lists available at ScienceDirect

Biochemical and Biophysical Research Communications

journal homepage: www.elsevier.com/locate/ybbrc

Mitochondrial NADP$^+$-dependent isocitrate dehydrogenase knockdown inhibits tumorigenicity of melanoma cells

Sung Hwan Kim [a], Young Hyun Yoo [b], Jin Hyup Lee [c], Jeen-Woo Park [a,*]

[a] School of Life Sciences, BK21 Plus KNU Creative BioResearch Group, College of Natural Sciences, Kyungpook National University, Taegu 702-701, Republic of Korea
[b] Mitochondria Hub Regulation Center, Dong-A University College of Medicine, Busan, Republic of Korea
[c] Department of Food and Biotechnology, Korea University, Sejong, Republic of Korea

ARTICLE INFO

Article history:
Received 17 July 2014
Available online 31 July 2014

Keywords:
Antioxidant enzyme
Melanoma
Tumorigenesis
Redox status
Angiogenesis

ABSTRACT

The potent cytotoxicity of reactive oxygen species (ROS) can cause various diseases but may also serve as a powerful weapon capable of destroying cancer cells. Although the balance between generation and elimination of ROS is maintained by the proper function of antioxidative systems, the severe disturbance of cellular redox status may cause various damages, leading to cell death. Mitochondrial NADP$^+$-dependent isocitrate dehydrogenase (IDH2), an NADPH-generating enzyme, is one of the major antioxidant and redox regulators in mitochondria. To assess the effect of IDH2 knockdown in the malignancy process, we generated B16F10 melanoma cells stably transfected either with the cDNA for mouse IDH2 cloned in antisense orientation or with a control vector. Mice injected with B16F10 cells harboring IDH2 downregulation showed a dramatic reduction in tumor progression in comparison to mice administered control cells. This effect might be secondary to a shift from a reducing to an oxidative state in tumor cells. The tumor tissue of mice administered B16F10 cells transfected with the IDH2 cDNA exhibited induction of apoptosis and downregulation of angiogenesis markers. These observations demonstrate that reduction of IDH2 levels in malignant cells has anti-tumorigenic effects and suggest that IDH2 is a potential target for cancer therapy.

1. Introduction

The balance of reactive oxygen species (ROS) formation and levels of antioxidative defenses is crucial for cell survival and growth, and it is critical for cells to remove ROS in order to remain viable and maintain their functions [1]. Therefore, a severe disruption of cellular redox status induces elevation of ROS levels, leading to cytotoxicity, inhibition of cell proliferation, and cell death. Not surprisingly, ROS production to trigger tumor cell death is a mechanism shared by all non-surgical cancer therapies, such as chemotherapy, radiotherapy, and photodynamic therapy [2].

A complex network of enzymatic and non-enzymatic antioxidant systems eliminates ROS and maintains cellular redox homeostasis. In addition to enzymes that directly remove ROS, enzymes providing essential reducing equivalents play a major role in maintaining cellular redox balance [3,4]. Reduced glutathione (GSH) protects from oxidative stress owing to its potent antioxidant functions and by providing a substrate for the mitochondrial glutathione peroxidase and glutathione-dependent phospholipid hydroperoxidase [5]. GSH levels in mitochondria are maintained by glutathione reductase, and NADPH is an essential reducing equivalent for enzyme-linked GSH recycling [6]. Furthermore, NADPH is required for the regeneration of the thioredoxin system, which is required to preserve cellular thiol homeostasis [7]. In this regard, mitochondrial NADPH acts as an essential component in the mitochondrial antioxidant system. Mitochondrial NAD$^+$-dependent isocitrate dehydrogenase (IDH2) catalyzes oxidative decarboxylation of isocitrate into α-ketoglutarate and the reduction of NADP$^+$ to NADPH. Recently, we reported that IDH2 is one of the major antioxidant and redox regulators, and prevents oxidative stress by producing NADPH in the mitochondria, since these organelles do not express glucose 6-phosphate dehydrogenase (G6PD) [8,9].

To assess the role of IDH2 in tumor progression, we stably transfected B16F10 mouse melanoma cells with the cDNA for mouse IDH2 cloned in an antisense orientation. We explored the tumorigenicity of B16F10 cells harboring IDH2 downregulation in mice, and we determined the molecular mechanism by which IDH2 downregulation suppresses tumor growth.

* Corresponding author. Fax: +82 53 943 2762.
E-mail address: parkjw@knu.ac.kr (J.-W. Park).

http://dx.doi.org/10.1016/j.bbrc.2014.07.105
0006-291X/

2. Materials and methods

2.1. Materials

β-$NADP^+$, isocitrate, xylenol orange, 2,4-dinitophenylhydrazine (DNPH), and 5,5′-dithiobis-(2-nitrobenzoic acid) (DTNB) were obtained from Sigma Chemical Co. (St. Louis, MO). Antibodies against cleaved lamin B, phospho-p53, Bcl-2, Bax, and VEGF were purchased from Santa Cruz Biotechnology (Santa Cruz, CA); Cleaved PARP, cleaved caspase-3, PUMA, phospho-Akt were purchased from Cell Signaling (Beverly, MA); p21, cytochrome c, and HIF-1α were purchased from Biosciences (San Diego, CA); Prx-SO3 was purchased from AB Frontier (Seoul, Korea). A peptide containing the 16 N-terminal amino acids of mouse IDH2 (ADKRIKVAKPVVEMPG) was used to prepare polyclonal anti-IDH2 antibodies [8].

2.2. Establishment of stably transfected cell lines

B16F10 mouse melanoma cells stably transfected with the cDNA for mouse IDH2 cloned in an antisense orientation were prepared as previously described [8]. B16F10 cells transfected with the LNCX vector backbone were used as a controls. B16F10 cells were cultured in Dulbecco's modified Eagle's medium containing 10% fetal bovine serum, 100 U/mL penicillin, and 100 μg/mL streptomycin at 37 °C in a 5% CO_2 atmosphere.

2.3. Enzyme assays

IDH2 activity was determined by measuring NADPH levels at 340 nm at 25 °C, as previously described [8]. To assess caspase-3 activity, tumor lysates (100 μg of protein) were added to the reaction buffer (100 mM HEPES, pH 7.4; 0.5 mM PMSF; 10 mM dithiothreitol; 1 mM EDTA; and 10% glycerol) containing the chromogenic peptide substrate Ac-DEVD-pNA (Calbiochem, San Diego, CA). Subsequently, reactions were incubated for 2 h at 37 °C, and absorbance was monitored at 405 nm to measure caspase activity.

2.4. Soft agar assay

In total, 1000 control or antisense IDH2-transfected B16F10 cells, suspended in 3 ml of 0.35% noble agar (growth medium with 10% fetal bovine serum), were spread evenly onto 60-mm plates covered with a 4-ml basal layer of 0.7% noble agar in Dulbecco's modified Eagle's medium. Subsequently, the plates were incubated in a humidified 37 °C incubator for 14 days, and growth medium was added onto the agar plate every 5 days. Colonies were visualized by staining with ρ-iodonitrotetrazolium violet overnight and counted.

2.5. Tumor formation assay

All experiments were carried out in 6-week-old male C57BL6 J mice obtained from Hyochang Science (Taegu, Korea). Animal studies were conducted in accordance with institutional guidelines for the care and use of laboratory animals. Control and antisense IDH2-transfected B16F10 cells (1×10^5/0.1 mL PBS) in the growth phase were subcutaneously injected into the right thigh of C57BL/6 mice. Four to six mice were used for each group. Tumor formation was monitored every two days and calculated (in mm^3) using width (x) and length (y) ($x^2y/2$, where $x < y$). Twenty-one days after the initial tumor inoculation, mice were euthanized and tumors were dissected and analyzed. Histological sections from one paraffin block per tumor were stained with hematoxylin and eosin (H & E) to assess tissue morphology.

2.6. Preparation of tissue extracts

Tumor tissue was homogenized at maximum speed for 15 s in a solution containing 0.3 M sucrose, 25 mM imidazole, 1 mM EDTA (pH 7.2), 8.5 μM leupeptin, and 100 μg/mL aprotinin. Subsequently, homogenates were centrifuged at 4000×g for 15 min at 4 °C, and the resulting supernatants were stored at −20 °C before use. Protein concentration was measured by the Bradford method using reagents purchased from Bio-Rad (Hercules, CA).

2.7. RNA isolation and reverse transcription (RT)-PCR

RNA was isolated using an RNeasy kit (Qiagen, Hilden, Germany), according to the manufacturer's instruction. Total RNA (1 μg) was reverse-transcribed using a first-strand cDNA synthesis kit (Invitrogen, Carlsbad, CA), according to the manufacturer's protocol. The cDNA template was amplified by RT-PCR by using a Perkin–Elmer GeneAmp PCR System 2400 (Perkin–Elmer Cetus, Waltham, MA), according to the manufacturer's protocol. Sequences of the primers used were as follows: *β-actin*, forward 5′-TCTACAATGAGCTGCGTGTG-3′, reverse 5′-ATCTCCTTCTGCATCCT-GTC-3′; *IDH2*, forward 5′-ATCAAGGAGAAGC-TCATCCTGC-3′, reverse 5′-TCTGTGGCCTTGTACTGGTCG-3′. β-actin expression was used as an internal control. The amplified DNA products were resolved on a 1% agarose gel and stained with ethidium bromide.

2.8. Immunoblot analysis

Proteins were separated on 10–12.5% SDS–polyacrylamide gel, transferred to nitrocellulose membranes, and subsequently subjected to immunoblot analysis using appropriate antibodies. Immunoreactive antigens were then detected with an enhanced chemiluminescence detection kit (Amersham Pharmacia Biotech, Buckinghamshire, UK).

2.9. Measurement of cellular redox status and oxidative damage

NADPH was measured using the enzymatic cycling method as described by Zerez et al. [10] and expressed as the ratio of NADPH to the total NADP pool. Intracellular H_2O_2 concentration was measured using the ferric sensitive dye xylenol orange, as previously described [11]. Thiobarbituric acid-reactive substances (TBARS) were determined as an independent measure of lipid peroxidation. Malondialdehyde (MDA) production was assessed with a TBARS spectrophotometric assay [12]. The protein carbonyl content was determined immunochemically using the OxyBlot Protein Oxidation Detection Kit (Millipore, Billerica, MA). The concentration of total glutathione was determined by the rate of formation of 5-thio-2-nitrobenzoic acid at 412 nm ($\varepsilon = 1.36 \times 10^4\ M^{-1}\ cm^{-1}$), and oxidized glutathione (GSSG) was measured by the DTNB–GSSG reductase recycling assay after treating GSH with 2-vinylpyridine [12].

2.10. Statistical analysis

The difference between two mean values was analyzed by Student's t-test and was considered to be statistically significant when $p < 0.05$.

3. Results and discussion

Mitochondrial NADPH is an essential reducing equivalent for the regeneration of antioxidant GSH and for the activity of NADPH-dependent thioredoxin system [6,7]. The latter is required for the activity of members of the mitochondrial thioredoxin

peroxidase family/peroxiredoxin family, such as peroxiredoxin III/protein SP-22 [13–15] and peroxiredoxin V/AOEB166 [16]. In this regard, the mitochondrial NADPH-generating enzyme IDH2 is critical for cellular defense against ROS-mediated damage and apoptosis.

To investigate the potential role of IDH2 in malignancies, we downregulated IDH2 expression in mouse melanoma B16F10 cells by stable transfection with an LNCX vector containing the mouse IDH2 cDNA in an antisense orientation. Cells stably transfected with the LNCX vector backbone were used as controls. IDH2 activity was ~50% lower in the antisense IDH2-transfected B16F10 cells than in control cells (Fig. 1A). Immunoblot analysis with an anti-IDH2 antibody and RT-PCR further confirmed the correlation between the levels of protein and mRNA, respectively, and the corresponding levels of enzyme activity (Fig. 1B and C). Another attribute of cancer cells that is not shared by normal cells is the ability to grow unanchored in soft agar [17]. After 2 weeks of culture in soft agar, antisense IDH2-transfected B16F10 cells formed fewer and smaller colonies than control cells (Fig. 1D and E). The level of peroxiredoxin (Prx)-SO_3, a marker for oxidative damage, were increased in B16F10 cells transfected with antisense IDH2 cDNA, indicating a shift to pro-oxidant cellular state in the context of IDH2 knockdown (Fig. 1F).

The effects of IDH2 downregulation on tumorigenicity were assessed in age-matched male mice subcutaneously injected with BF16F10 melanoma cells transfected with either the antisense IDH2 cDNA or control vector. Melanoma tumor growth was abrogated in mice harboring B16F10 cells transfected with the antisense IDH2 cDNA [IDH2(-)] compared to mice injected with control cells [control] (Fig. 2A and B). In addition, tumor weight was lower in IDH2(-) mice than in control mice (Fig. 2C). These *in vivo* results are consistent with our *in vitro* data, demonstrating that the IDH2 knockdown exerts anti-tumorigenic effects both *in vitro* and *in vivo*. Accordingly, histological analysis of tumor tissue harvested 3 weeks after injections showed extensive malignancy in control mice (Fig. 2D).

The activity of IDH2 was 40% lower in IDH2(-) tumor tissue than in control tumor tissue (Fig. 3A). In agreement with IDH2 downregulation, the ratio for mitochondrial [NADPH]/[$NADP^+$/NADPH] was lower in IDH2(-) tumor tissue than in control tumor tissue (Fig. 3B). Although moderate levels of ROS may function as signals to promote cell proliferation and survival, severe increase of ROS can induce cell death [18]. To determine whether differences in tumorigenicity observed in IDH2(-) and control tumor tissues were associated with ROS formation, the levels of intracellular H_2O_2 in tumor tissues were measured. IDH2(-) tumor tissue

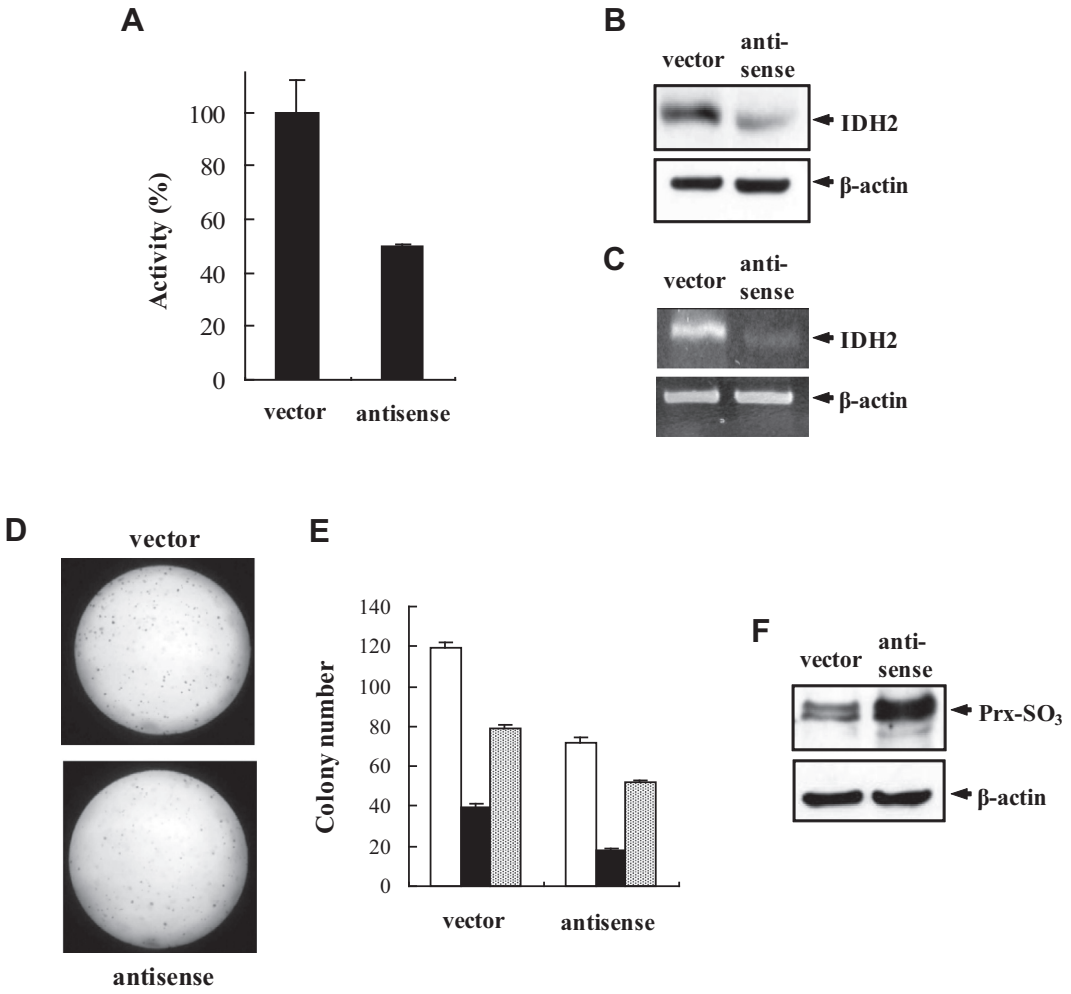

Fig. 1. Downregulation of IDH2 in B16F10 cells. (A) IDH2 activity of B16F10 cells transfected either with LNCX containing a mouse IDH2 cDNA cloned in an antisense orientation or with LNCX vector backbone (control). Each value represents the mean ± S.D. from three independent experiments. (B) Immunoblot analysis of IDH2 protein expressed in B16F10 transfected cells. β-Actin was used as a loading control. (C) RT-PCR analysis of IDH2 expression in B16F10 transfected cells. β-Actin was used as a control. (D) Representative dishes by soft agar assay. (E) Stained colonies counted and recorded as the total number of colonies (*open bar*), colonies greater than 130 (Image-J threshold) in size (*solid bar*), and colonies smaller than 130 in size (*gray bar*). Each value represents the mean ± S.D. from three independent experiments. (F) The oxidized Prx levels of the cell extracts were determined by anti-Prx-SO_3 antibody after SDS–PAGE.

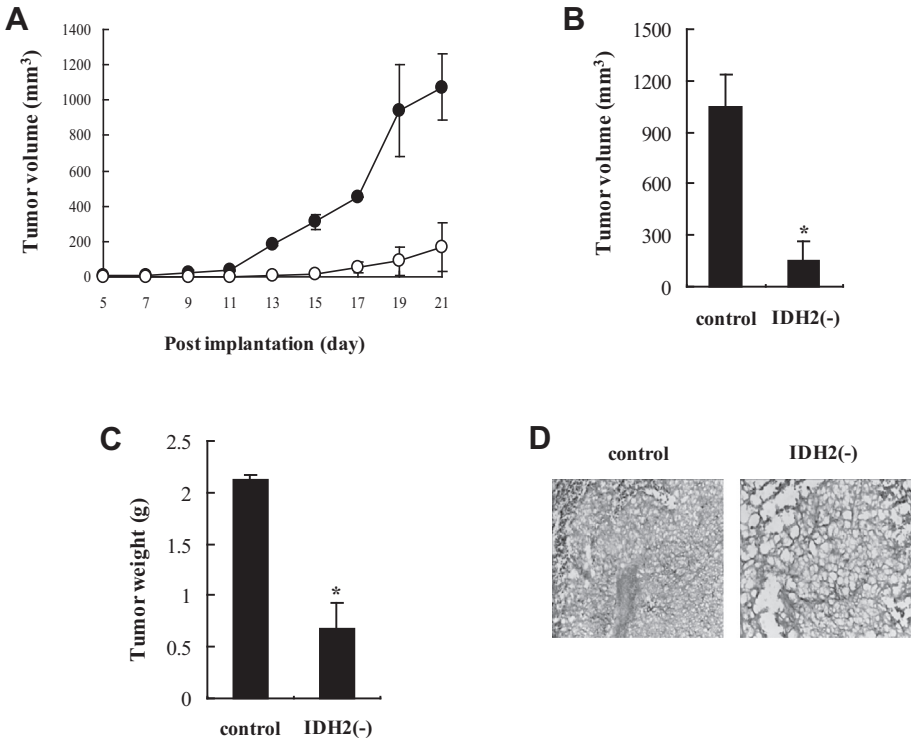

Fig. 2. B16F10 melanoma growth *in vivo*. (A) Growth curve showing the average melanoma size for mice harboring B16F10 cells transfected with the antisense IDH2 cDNA [IDH2(-)] and mice injected with control cells [control]. Tumor formation monitored every two days and calculated (in mm^3) using width (x) and length (y) ($x^2y/2$, where $x < y$). Each value represents the mean ± S.D. from 4 to 6 independent experiments. (B) Average volume of IDH2(-) and control tumors. Tumor volumes were determined at the time of sacrifice. Each value represents the mean ± S.D. from 4 to 6 independent experiments. $^*p < 0.01$ versus the control tumor. (C) Average weight of IDH2(-) and control tumors. Tumor weight was determined at the time of sacrifice. Each value represents the mean ± S.D. from 4 to 6 independent experiments. $^*p < 0.01$ versus the control tumor. (D) Tissue slices from IDH2(-) and control tumors were examined for morphological changes.

exhibited higher level of intracellular H_2O_2 than in control tumor tissue (Fig. 3C). Prx-SO_3 levels were higher in IDH2(-) tumor tissue than in control tumor tissue (Fig. 3D), confirming that the cellular redox balance is severely disturbed by IDH2 downregulation.

Under oxidative stress, excessive ROS are detrimental to lipid, protein, and DNA integrity, leading to severe and irreversible oxidative damage. Oxidation of protein side chains results in formation of carbonyl derivatives, a quantitative marker of protein oxidation and oxidative stress [19]. We tested whether oxidative protein damage increased in IDH2(-) tumor tissue. Levels of oxidative protein damage in tumor lysates were determined by measuring the amount of derivatized carbonyl groups on oxidized proteins by western blotting for oxidized protein carbonyl groups. Oxidative protein damage was higher in IDH2(-) tumor tissue than in control tumor tissue. TBARS spectrometric assay revealed that levels of lipid peroxidation were higher in IDH2(-) tumor tissue than in control tumor tissue (Fig. 3F).

The redox status and GSH/GSSG ratio are perturbed under multiple oxidative stress-induced conditions [20]. The ratio of GSSG/total GSH (GSH_t), which may reflect the efficiency of GSH turnover, was significantly higher in IDH2(-) tumor tissue than in control tumor tissue (Fig. 3G). This data indicate that GSSG was reduced less efficiently in IDH2(-) tumor tissue than in control tumor tissue. Protein S-glutathionylation is a post-translational modification of protein sulfhydryl groups that occurs under oxidative stress [21]. Western blot analysis of tumor lysates with an anti-GSH IgG revealed an increase of glutathionylated proteins in IDH2(-) tumor tissue (Fig. 3H). Taken together, these results indicate that elevated steady-state level of ROS in tumor cells may lead to oxidative damage.

To determine whether the inhibition of tumorigenesis by downregulation of IDH2 is associated with induction of apoptosis, we assayed apoptosis-related factors in IDH2(-) and control tumor tissues. Caspase-3 activation in the IDH2(-) and control tumor tissues was assessed by caspase colorimetric assay. Caspase-3 activity was significantly increased by knockdown of IDH2 (Fig. 4A). Western blot analysis revealed that apoptotic marker protein expression was higher in IDH2(-) tumor tissue than in control tumor tissue (Fig. 4B). At higher ROS levels, cell division is arrested, and this effect is prolonged, cells undergo apoptosis [22]. Oxidative stress activated p53, which binds to DNA and induces the expression of multiple genes such as p21, a protein that arrests cancer cells in the G_1 phase and modulates the kinase activities of various cyclin-dependent kinases [23,24]. Western blot analysis revealed that p21 and phosphorylated p53 levels were increased in IDH2(-) tumor tissue compared to those in control tumor tissue (Fig. 4C).

The heterodimeric transcription factor HIF-1 (hypoxia-inducible factor 1) mediates the response to hypoxia. HIF-1 controls expression of multiple genes of pivotal importance for cellular metabolism, angiogenesis, cell cycle regulation, and inhibition of apoptosis [25]. Protein levels of HIF-1α in IDH2(-) and control tumor tissues were examined by immunoblotting. HIF-1α accumulation was reduced in IDH2(-) tumor tissue compared to that in control tumor tissue. Accordingly, expression of VEGF, a known target of HIF-1α was suppressed in IDH2(-) tumor tissue (Fig. 4D). Regulation of HIF-1 stability and function under hypoxic conditions, as well as under stimulation by growth factors, is modulated by the phosphatidylinositol 3-kinase (PI3K)-protein kinase B (PKB/Akt) signaling pathway [26]. Akt, a serine-threonine kinase and downstream target of PI3K, is regulated by phosphoinositide-dependent protein kinases (PDKs) [27]. Akt phosphorylation was

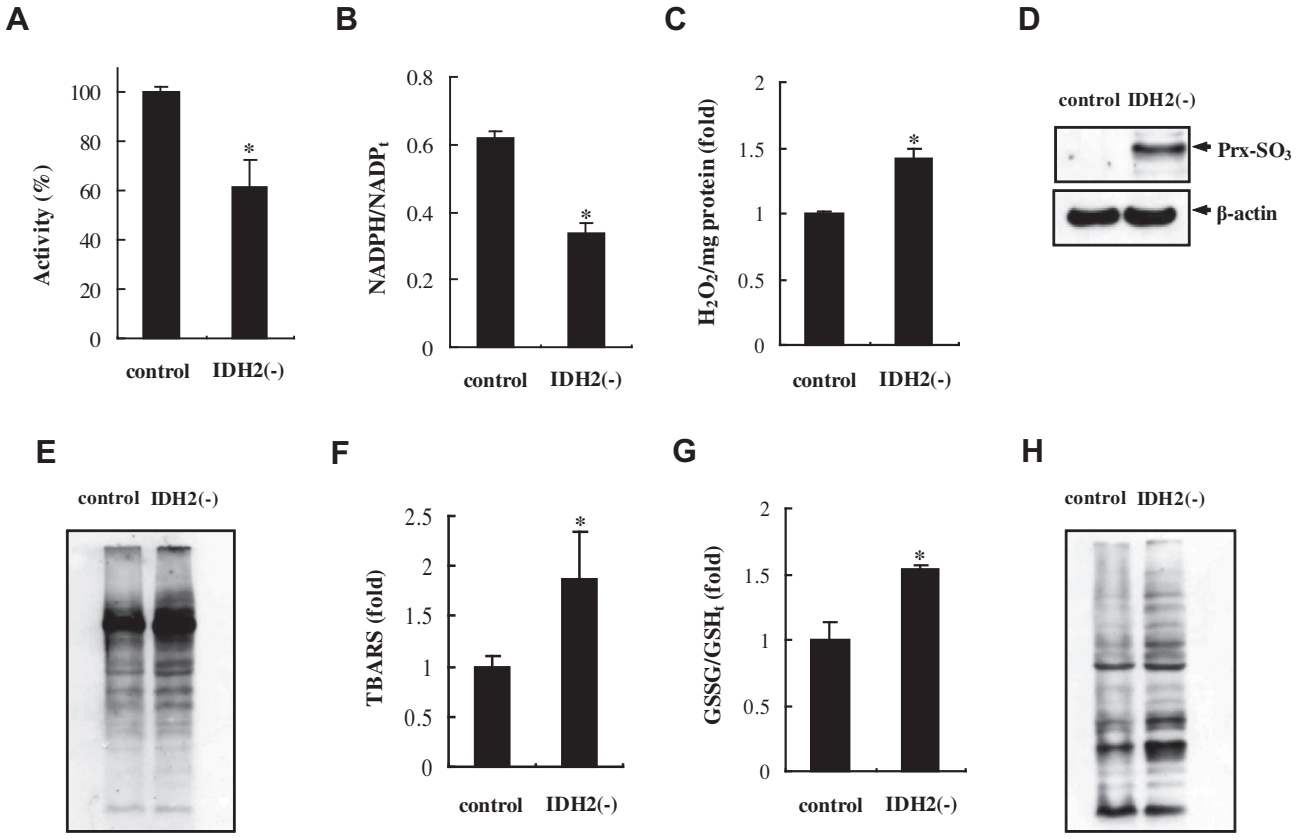

Fig. 3. Redox status and oxidative damage in IDH2(-) and control tumor tissues. (A) IDH2 activity is expressed as a percentage of the control value. (B) Ratio of NADPH versus the total NADP pool in the tumor tissue extracts. (C) Production of H_2O_2 in the tumor tissue extracts was measured with xylenol orange. (A–C) Each value represents the mean ± S.D. from 4 to 6 independent experiments. $^*p < 0.01$ versus the control tumor tissue. (D) The oxidized Prx levels in tumor lysates were determined by SDS–PAGE with anti-Prx-SO_3 antibody. (E) DNP adducts in the tumor tissue extracts were monitored with an anti-DNP antibody. (F) The level of MDA accumulated in tumor tissue extracts was determined using a TBARS assay. Each value represents the mean ± S.D. from 4 to 6 independent experiments. $^*p < 0.01$ versus the control tumor tissue. (G) GSSG versus total GSH pool in the tumor tissue extracts. Each value represents the mean ± S.D. from 4 to 6 independent experiments. $^*p < 0.01$ versus the control tumor tissue. (H) Glutathionylated adducts in the tumor tissue extracts were monitored with an anti-GSH antibody.

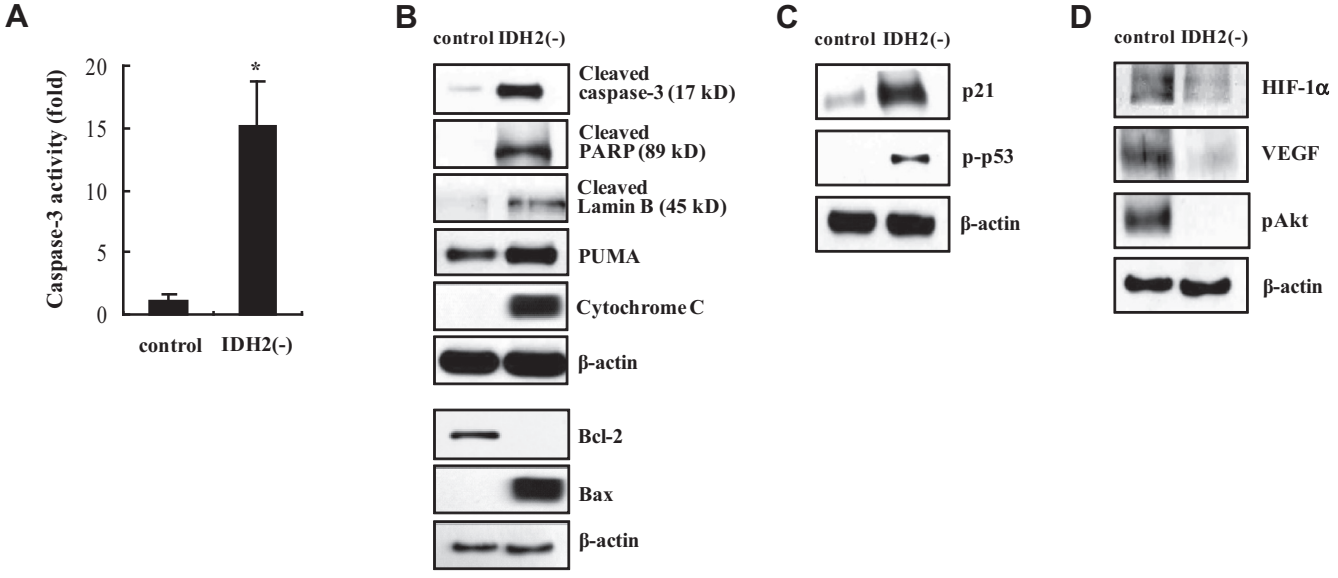

Fig. 4. Modulation of tumorigenesis marker expression in IDH2(-) and control tumor tissues. (A) Activation of caspase-3 in the tumor tissue extracts. Protease activity of caspase-3 was calculated by monitoring the absorbance at 405 nm. Each value represents the mean ± S.D. from 4 to 6 independent experiments. $^*p < 0.01$ versus the control tumor tissue. Tumor lysates containing equal amounts of protein (20 μg) were separated by SDS–PAGE and then subjected to immunoblot analysis using antibodies specific for apoptosis (B), cell cycle (C), and angiogenesis markers (D).

lower in IDH2(-) tumor tissue was than in control tumor tissue (Fig. 4D).

In the present study, we demonstrated that downregulation of the mitochondrial NADPH-generating enzyme IDH2 inhibits tumor growth both *in vitro* and *in vivo*, presumably through the induction of apoptosis and downregulation of angiogenesis-related factors. These observations provide direct evidence that the reduction of IDH2 levels in malignant cells has anti-tumorigenic effects and suggest that IDH2 is a potential target for cancer therapy.

Acknowledgments

This research was supported by National Research Foundation (NRF) of Korea Grants funded by the Korean Government (2014001483, 2014000455 and 2013004950).

References

[1] J. Fang, T. Seki, H. Maeda, Therapeutic strategies by modulating oxygen stress in cancer and inflammation, Adv. Drug Deliv. Rev. 61 (2009) 290–302.
[2] J. Wang, J. Yi, Cancer cell killing via ROS, Cancer Biol. Ther. 7 (2008) 1875–1884.
[3] J.M. Mates, Effects of antioxidant enzymes in the molecular control of reactive oxygen species toxicology, Toxicology 153 (2000) 83–104.
[4] I.S. Kil, S.W. Shin, H.S. Yeo, Y.S. Lee, J.-W. Park, Mitochondrial NADP$^+$-dependent isocitrate dehydrogenase protects cadmium-induced apoptosis, Mol. Pharmacol. 70 (2006) 1053–1061.
[5] A.M. Avery, S.A. Willetts, S.V. Avery, Genetic dissection of the phospholipid hydroperoxidase activity of yeast gpx3 reveals its functional importance, J. Biol. Chem. 279 (2004) 46652–46658.
[6] M. Kirsch, H. de Groot, NAD(P)H, a directly operating antioxidant?, FASEB J 15 (2001) 1569–1574.
[7] H. Nakamura, Thioredoxin and its related molecules: update 2005, Antioxid. Redox Signal. 7 (2005) 823–828.
[8] S.H. Jo, M.K. Son, H.J. Koh, S.M. Lee, I.H. Song, Y.O. Kim, Y.S. Lee, K.S. Jeong, W.B. Kim, J.W. Park, B.J. Song, T.L. Huh, Control of mitochondrial redox balance and cellular defense against oxidative damage by mitochondrial NADP$^+$-dependent isocitrate dehydrogenase, J. Biol. Chem. 276 (2001) 16168–16176.
[9] J.H. Lee, S.Y. Kim, I.S. Kil, J.-W. Park, Regulation of ionizing radiation-induced apoptosis by mitochondrial NADP$^+$-dependent isocitrate dehydrogenase, J. Biol. Chem. 282 (2007) 13385–13394.
[10] C.R. Zerez, S.J. Lee, K.R. Tanaka, Spectrophotometric determination of oxidized and reduced pyridine nucleotides in erythrocytes using a single extraction procedure, Anal. Biochem. 164 (1987) 367–373.
[11] Z.Y. Jiang, J.V. Hunt, S.P. Wolff, Ferrous ion oxidation in the presence of xylenol orange for detection of lipid hydroperoxide in low density lipoprotein, Anal. Biochem. 202 (1992) 384–389.
[12] J.K. Tak, J.-W. Park, The use of ebselen for radioprotection in cultured cells and mice, Free Radic. Biol. Med. 46 (2009) 1177–1185.
[13] M. Araki, H. Nanri, K. Ejima, Y. Murasato, T. Fujiwara, Y. Nakashima, M. Ikeda, Antioxidant function of the mitochondrial protein SP-22 in the cardiovascular system, J. Biol. Chem. 274 (1999) 2271–2278.
[14] S.W. Kang, H.Z. Chae, M.S. Seo, K. Kim, I.C. Baines, S.G. Rhee, Mammalian peroxiredoxin isoforms can reduce hydrogen peroxide generated in response to growth factors and tumor necrosis factor-alpha, J. Biol. Chem. 273 (1998) 6297–6301.
[15] S. Watabe, H. Hasegawa, K. Takimoto, Y. Yamamoto, S. Takahashi, Possible function of SP-22, a substrate of mitochondrial ATP-dependent protease, as a radical scavenger, Biochem. Biophys. Res. Commun. 213 (1995) 1010–1016.
[16] B. Knoops, A. Clippe, C. Bogard, K. Arsalane, R. Wattiez, C. Hermans, E. Duconseille, P. Falmagne, A. Bernard, Cloning and characterization of AOEB166, a novel mammalian antioxidant enzyme of the peroxiredoxin family, J. Biol. Chem. 274 (1999) 30451–30458.
[17] M.H. Yoo, X.M. Xu, B.A. Carlson, V.N. Gladyshev, D.L. Hatfield, Thioredoxin reductase 1 deficiency reverses tumor phenotype and tumorigenicity of lung carcinoma cells, J. Biol. Chem. 281 (2006) 13005–13008.
[18] M. Nishikawa, Reactive oxygen species in tumor metastasis, Cancer Lett. 266 (2008) 53–59.
[19] R.T. Dean, S. Fu, R. Stocker, M.J. Davis, Biochemistry and pathology of radical-mediated protein oxidation, Biochem. J. 324 (1997) 1–18.
[20] S. Bharath, M. Hsu, D. Kaur, S. Rajagopalan, J.K. Andersen, Glutathione, iron and Parkinson's disease, Biochem. Pharmacol. 64 (2002) 1037–1048.
[21] Y.C. Chai, S.S. Ashraf, K. Rokutan, R.B. Johnston, J.A. Thomas, S-thiolation of individual human neutrophil proteins including actin by stimulation of the respiratory burst: evidence against a role for glutathione disulfide, Arch. Biochem. Biophys. 310 (1994) 273–281.
[22] W.C. Burhans, N.H. Heintz, The cell cycle is a redox cycle: linking phase-specific targets to cell fate, Free Radic. Biol. Med. 47 (2009) 1282–1293.
[23] A. Zetterberg, O. Larsson, K.G. Wiman, What is the restriction point?, Curr Opin. Cell Biol. 7 (1995) 835–842.
[24] Y. Yu, Z. Kovacevic, D.R. Richardson, Tuning cell cycle regulation with an iron key, Cell Cycle 6 (2007) 1982–1994.
[25] A. Galanis, A. Pappa, A. Giannakakis, E. Lanitis, D. Dangaj, R. Sandaltzopoulos, Reactive oxygen species and HIF-1 signalling in cancer, Cancer Lett. 266 (2008) 12–20.
[26] R.J. Shaw, L.C. Cantly, Ras, PI(3)K and mTOR signalling controls tumour cell growth, Nature 441 (2006) 424–430.
[27] D.R. Alessi, S.R. James, C.P. Downes, A.B. Holmes, P.R. Gaffney, C.B. Reese, P. Cohen, Characterization of a 3-phosphoinositide-dependent protein kinase which phosphorylates and activates protein kinase B, Curr. Biol. 7 (1997) 261–269.